Optically engineered quantum interference of delocalized wave functions in a bulk solid: The example of solid *para*-hydrogen

Hiroyuki Katsuki,[1,2,*] Yosuke Kayanuma,[3,4] and Kenji Ohmori[1,2,4,†]

[1]*Institute for Molecular Science, National Institutes of Natural Sciences, Myodaiji, Okazaki 444-8585, Japan*
[2]*SOKENDAI (The Graduate University for Advanced Studies), Okazaki 444-8585, Japan*
[3]*Research Organization for the 21st Century, Osaka Prefecture University, Sakai 599-8531, Japan*
[4]*CREST, Japan Science and Technology Agency, Kawaguchi, Saitama 332-0012, Japan*

Local excitations of indistinguishable particles in a solid are quantum-mechanically superposed to give delocalized wave functions. Their interference is often so short-lived that it eludes observation and manipulation. Here we have actively controlled interference of delocalized vibrational wave functions in solid *para*-hydrogen produced by a pair of ultrashort laser pulses. The ultrafast evolution of their interference changes from almost completely constructive (amplification by a factor of ∼4) to destructive when we change the timing of those two laser pulses by only 4 fs. This active control serves as an experimental tool to investigate the spatiotemporal evolution of a wave function in a bulk solid.

I. INTRODUCTION

A specific type of excitation of solids including the Frenkel exciton could generate a delocalized quantum state, in which local excitations of indistinguishable particles in a solid are quantum-mechanically superposed to give a delocalized wave function.[1,2] Interference of such delocalized local excitations is a direct signature of the delocalized wave nature in a solid but is often so short lived that, to date, it had eluded observation and manipulation. Here we demonstrate actively controlled quantum interference of those delocalized wave functions in a bulk solid.

Coherent control is a technique that uses coherent light to manipulate the interference of wave functions.[3,4] It is a basic way of controlling a variety of quantum systems and has been exemplified for electronic, vibrational, and rotational states of atoms and molecules,[5–18] excitons and spins in the solid state,[19–24] and translational motions of atoms in Bose-Einstein condensate.[25] Here we apply this technique to delocalized local excitations in a bulk solid.

We take vibrons of solid *para*-hydrogen (*p*-H$_2$) as an example of delocalized local excitations in a bulk solid.[1,2] *Para*-hydrogen is the hydrogen molecule whose nuclear spin function is antisymmetric under the permutation of protons. Only even rotational quantum number J is allowed for *p*-H$_2$ according to Pauli's exclusion principle that requires the total wave function to be antisymmetric under the permutation of Fermi particles. Most of the *p*-H$_2$ molecules are thermally populated in $J = 0$ in the solid state. The isotropy of this $J = 0$ wave function does not induce any electrostatic multipole-multipole interactions, giving extremely weak intermolecular interactions. The rotational and vibrational quantum numbers, J and v, thus remain well-defined even in a solid, and each molecule in solid *p*-H$_2$ is safely assumed to be freely rotating and vibrating.[26,27] Because of these properties, solid *p*-H$_2$ is considered as one of the simplest molecular crystals, and its vibrons are well known to be "the simplest and most perfect examples of Bloch states in all of solid-state physics."[26]

There have been many high-resolution spectroscopic studies of ro-vibrational transitions in solid *p*-H$_2$ (Refs. 26–29).

Some measurements have been made of its coherence lifetime;[30–32] the vibrational coherence lifetime of $v = 1$ has been reported to be ∼100 ns.[31] Here we demonstrate direct observation and manipulation of quantum interference of these $v = 1$ vibrons in *p*-H$_2$ that could be resistant to decoherence in its bulk-solid environment.[28]

This paper is organized as follows. In Sec. II, the vibron wave function in solid *p*-H$_2$ is formulated. The experimental details are described in Sec. III. The experimental results and discussions are presented in Sec. IV. Concluding remarks are given in Sec. V.

II. VIBRONS IN SOLID PARAHYDROGEN

It is experimentally verified in previous spectroscopic studies that the absorption peak of solid *p*-H$_2$ around 4150 cm^{-1} has finite bandwidth of ∼5 cm^{-1} (Ref. 33), and this corresponds to the band structure composed of multiple vibrons ($v = 1$, **k**) with different **k** values, where **k** is the wave vector of the vibron.[26] Based on these previous spectroscopic studies, it is thus well established that the wave functions of these vibrons are delocalized over a single *p*-H$_2$ crystal. Figure 1(a) describes how this delocalized vibron is formed from vibrationally excited states of isolated molecules. We start with an ensemble of n noninteracting *p*-H$_2$ molecules, one of which is vibrationally excited to $v = 1$. This gives n energetically degenerate wave functions, each of which is spatially localized and given by

$$|v_i = 1\rangle \equiv \prod_{j \neq i}^{n} |v_i = 1, J = 0\rangle |v_j = 0, J = 0\rangle, \quad (1)$$

where v_i represents the vibrational quantum number of the ith molecule. The rotational quantum number J is hereafter omitted for simplicity. When the molecules form a crystal, the interaction among these locally excited states gives a vibron with the Frenkel Hamiltonian[1] given by

$$H = \sum_i \epsilon_i |v_i = 1\rangle\langle v_i = 1| + \sum_{i, j \neq i} V_{ij} |v_i = 1\rangle\langle v_j = 1|, \quad (2)$$
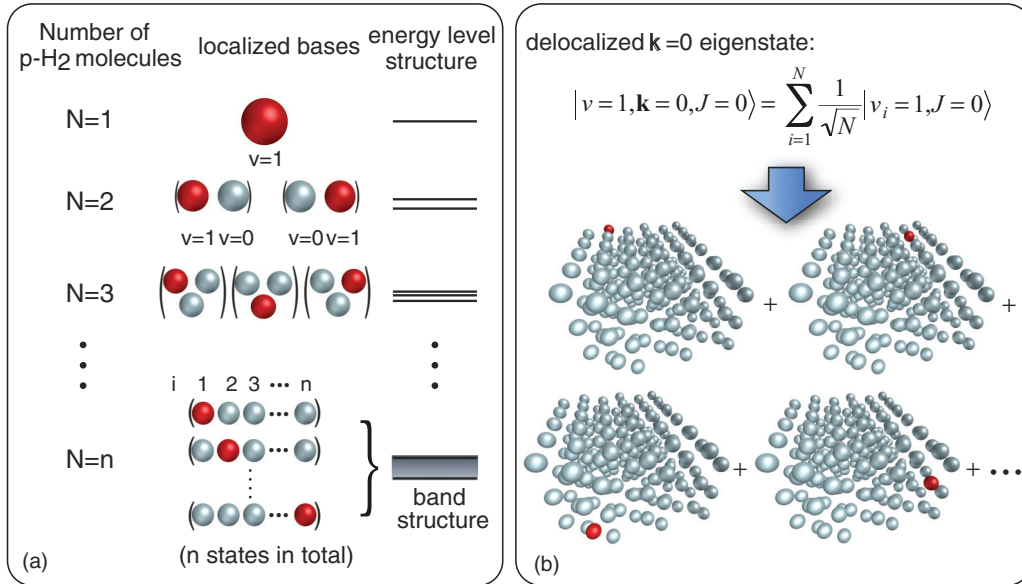
FIG. 1. (Color) Formation of the delocalized vibron in solid p-H_2. (a) A band structure arises from the interaction among many indistinguishable p-H_2 molecules, one of which is vibrationally excited. The red and blue spheres stand for the vibrationally excited and ground-state p-H_2 molecules, respectively. (b) Every p-H_2 molecule within a single crystal has an equal probability to be vibrationally excited. These locally excited states $|v_i = 1\rangle$ ($i = 1, \ldots, N$) are coherently superposed to give a delocalized vibron state $|v = 1, \mathbf{k} = 0\rangle$.

where ϵ_i is the energy of the locally excited state and V_{ij} is the vibron-hopping interaction.[29] This Hamiltonian matrix is diagonalized, so that the degeneracy is lifted to give the band structure composed of delocalized vibrational eigenfunctions $|v = 1, \mathbf{k}\rangle$ with different $\mathbf{k}$ values.[33,34] Within this band structure of different $\mathbf{k}$ states, Raman excitation that we employ in this study is safely assumed to be allowed only to the $\mathbf{k} = 0$ state,

$$|v = 1, \mathbf{k} = 0\rangle = \sum_i^N \frac{1}{\sqrt{N}} |v_i = 1\rangle, \qquad (3)$$

in which localized $v = 1$ states at different sites in a single p-H_2 crystal are coherently superposed, as schematically shown in Fig. 1(b).

III. EXPERIMENT

Normal H_2 was converted to p-H_2 with a ferromagnetic catalyst [FeO(OH)] at $\sim$17 K and stored in a stainless cylinder at room temperature. Gas-phase p-H_2 was slowly introduced through a stainless tube into a copper cell (diameter 25 mm, length 8 mm, windows BaF_2) attached to a brass cold plate fixed in the liquid-He open-cycle cryostat (Universal Cryogenics IRLMED07). The temperature of the cell was controlled between 9.2 K and 9.7 K during the crystallization of p-H_2, which took about 50 min to fill the copper cell, and then lowered slowly to 5.4 K. The crystal grew radially inwards from the inner surface of the copper cell. It is known from previous spectroscopic studies[29] that the crystal thus prepared has the hexagonal close-packed structure with its c axis pointing along the radial direction of the sample cell. The crystal was totally transparent without any visible cracks, as shown in Fig. 2(a). The *ortho/para* ratio in the crystal was

estimated to be $\sim$4.0 $\times$ 10^{-3} from the absorption intensity of the $v = 1$ vibron band.[35]

The scheme of the current experiment is shown in Fig. 2(b). The coherence between the ground state $|v = 0\rangle$ and the delocalized vibron state $|v = 1, \mathbf{k} = 0\rangle$ was generated with the femtosecond (fs) pump and Stokes pulses (pulse widths $\sim$30 and $\sim$110 fs, respectively), hereafter referred to as an "impulsive-Raman-excitation pair" (IREP), whose wavelengths were tuned to $\sim$595 and $\sim$796 nm, respectively. Here the term *impulsive* stands for simultaneous irradiation of pump and Stokes pulses.

The pump and Stokes pulses were prepared with a homemade two-stage noncollinear optical parametric amplifier and a Ti:sapphire regenerative amplifier, respectively, driven at a repetition rate of 1 kHz. The delay between these pump and Stokes pulses was tuned with a motorized stage so that the excitation efficiency was maximized, accordingly close to zero in the present IRE scheme in which no resonant intermediate state was employed. The IREP was introduced collinearly into a homemade highly stabilized Michelson interferometer to generate a pair of IREPs with their delay τ_{IRE} stabilized and controlled on the attosecond time scale.

Figure 3 schematically describes our interferometer. The delay τ_{IRE} was tuned coarsely with a motorized stage (Newport M-ILS100PP), whereas it was fine-tuned with a piezo stage (PI P-752.11C); both of those stages were inserted into one arm of the interferometer. Details of the stabilization of τ_{IRE} are given in Sec. IV. The pump pulses were separated from the Stokes pulses with a dichroic mirror after the interferometer, and those four pulses of two IREPs were focused into the p-H_2 crystal with an off-axis parabolic mirror to induce quantum interference of the delocalized vibron.

The probe pulse was prepared with an optical parametric amplifier (Spectra Physics TOPAS) whose output was tuned
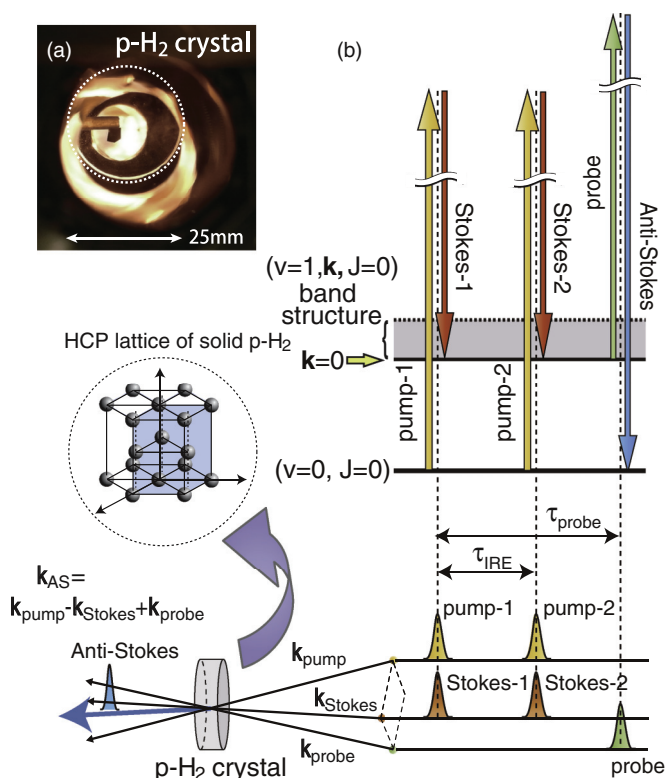
FIG. 2. (Color) Experimental scheme. (a) Snapshot of the p-H_2 crystal grown in the cryostat. The dotted circle indicates the p-H_2 crystal. (b) A sequence of the laser pulses employed in the present study to observe and control the interference of the delocalized vibron state $|v = 1, \mathbf{k} = 0\rangle$. The delay τ_{IRE} between the first and second pairs of the pump and Stokes pulses is stabilized and controlled on the attosecond time scale, and the coherence which remains after the second pump-Stokes pair is observed by measuring the intensity of the anti-Stokes beam induced by the probe pulse.

to ∼550 nm with its temporal width of ∼60 fs. Its spectral bandwidth was reduced with a slit combined with a single grating stretcher and compressor, so that its temporal width was elongated to ∼1 ps. This elongated pulse was used as a probe pulse to induce anti-Stokes scattering around 450 nm. As shown in Fig. 2(b), the folded-boxcars geometry was employed with the present three-color pump, Stokes, and probe pulses. Their wave vectors and angular frequencies are hereafter denoted as $\mathbf{k}_{pump}$ and ω_{pump}, $\mathbf{k}_{Stokes}$ and ω_{Stokes}, and $\mathbf{k}_{probe}$ and ω_{probe}, respectively. The coherent anti-Stokes beam with its wave vector $\mathbf{k}_{AS} = \mathbf{k}_{pump} - \mathbf{k}_{Stokes} + \mathbf{k}_{probe}$ and its angular frequency $\omega_{AS} = \omega_{pump} - \omega_{Stokes} + \omega_{probe}$ was spatially and energetically discriminated from the pump, Stokes, and probe pulses, and its intensity was measured with a CCD camera (Andor Newton DU-940BU) attached to a spectrometer (TII M-3501i), whose outputs were accumulated for 0.5 s over 500 probe-laser shots to give each data point shown in the present paper. The intensity of the anti-Stokes beam thus measured is proportional to the square of the coherence between the ground and $\mathbf{k} = 0$ vibron states, which is defined to be the off-diagonal element of their density matrix. Each of the pulse energies of the pump, Stokes, and probe pulses was less than 0.1 μJ/pulse. The temperature of the crystal was kept constant

at 5.3 K–5.4 K during the measurements, not affected by the irradiation of the laser pulses.

IV. RESULTS AND DISCUSSIONS

The quantum state prepared by two IREPs is given by

$$|\Psi(t, \tau_{IRE})\rangle = |v = 0\rangle + c|v = 1, \mathbf{k} = 0\rangle e^{-i\omega_1 t}(1 + e^{i\omega_1 \tau_{IRE}}),$$

$$(4)$$

where $c (\ll 1)$ is the amplitude of the Raman excitation, $|v = 0\rangle$ is the ground-state wave function given by $|v = 0\rangle \equiv \prod_i |v_i = 0\rangle$, and ω_1 is the angular frequency between $|v = 0\rangle$ and $|v = 1, \mathbf{k} = 0\rangle$ states. It is seen from Eq. (4) that the coherence between $|v = 0\rangle$ and $|v = 1, \mathbf{k} = 0\rangle$ states oscillates with a period of $2\pi/\omega_1$ as a function of τ_{IRE}.

Figure 4(a) shows the intensity of the anti-Stokes beam measured at ∼448.7 nm of the spectrometer and plotted as a function of the delay τ_{IRE} between two IREPs scanned with the piezo stage of the interferometer around 10 ps in steps of ∼120 as with the probe delay τ_{probe} fixed to ∼1 ns. The full range of each abscissa τ_{IRE} of Fig. 4 was calibrated with a reference interferogram of cw He-Ne laser beams measured with a photodiode simultaneously with the vibron interferogram. Those He-Ne laser beams traveled in the interferometer along their optical paths aligned ∼5 mm below those of IREPs. A sine function was fitted to the reference He-Ne interferogram, and the period of that fitted sine function was calibrated to be $T = c_0/\lambda$, where c_0 is the speed of light and $\lambda = 632.991$ nm is the wavelength of the He-Ne laser beam in vacuum. The correction thus made to the full range was less than ∼1% of the full range estimated from the piezo movement.

The intensity increases and decreases alternately, showing a clear beat. A sine curve fitted to the measured beat gives its oscillation period to be 8.05 fs. This value agrees well with a value 8.04 fs deduced from the energy spacing $\omega_1 = 4149.75$ cm^{-1} reported in a previous spectroscopic study for the ground state $|v = 0\rangle$ and the vibron state $|v = 1, \mathbf{k} = 0\rangle$ (Ref. 28). It is reasonably concluded, therefore, that the beat shown in Fig. 4(a) is the quantum interferogram of the $\mathbf{k} \simeq 0$ vibron delocalized over a single p-H_2 crystal. We have thus observed the interference of delocalized local excitations in a bulk solid for the first time. The dashed horizontal line represents the intensity of the anti-Stokes beam arising from a single IRE, which is averaged between two IREPs produced by the interferometer. The intensity given by the first IREP should be amplified by the second IREP by a factor of 4 when the interference is perfectly constructive, since the amplitude of the $\mathbf{k} = 0$ wave function is doubled, and its modulus square is measured with the probe pulse. It is seen in Fig. 4(a) that the ratio of the maximum of the interferogram to the level of the dashed line, hereafter referred to as a coherent factor, is ∼4, indicating that the interference is almost complete. It is also seen that the destructive interference suppresses the signal. The fringe contrast of the interferogram, defined to be $(I_+ - I_-)/(I_+ + I_-)$, where I_+ and I_- are the maximum and the minimum of the fitted sine function, is better than 0.99 for Fig. 4(a). Figure 4(b) shows another interferogram measured by scanning τ_{IRE} around 500 ps. The coherent factor remains ∼4, showing that the coherence is almost
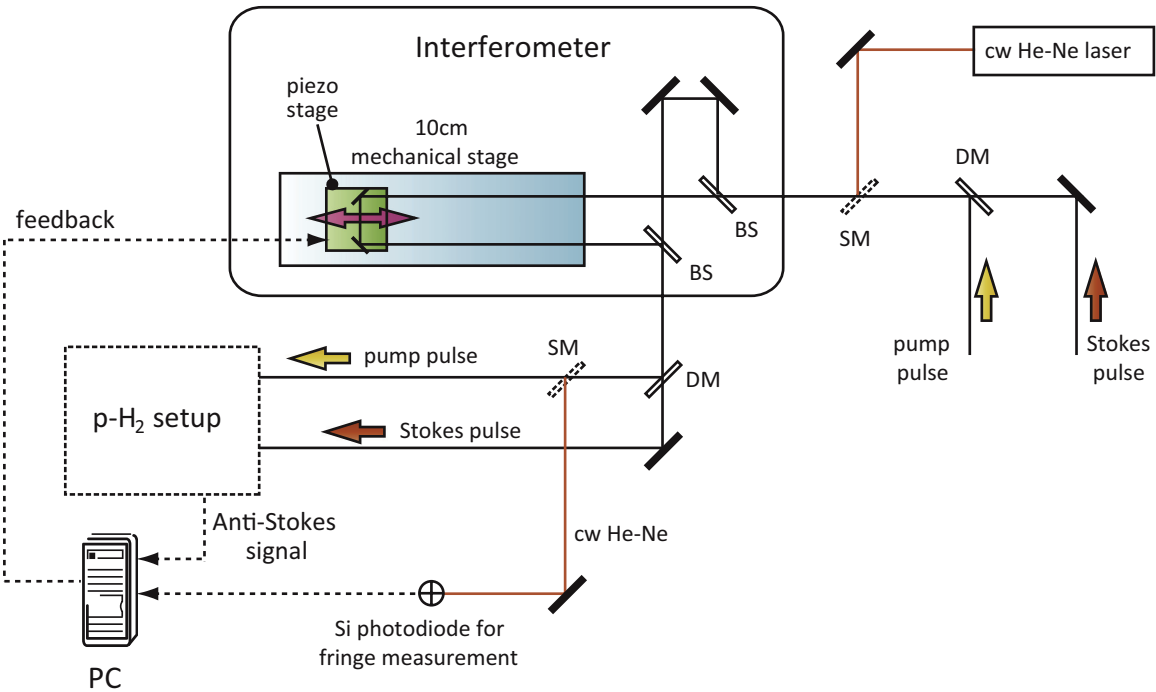
FIG. 3. (Color online) Optical setup for a highly stabilized Michelson interferometer. DM, dichroic mirror; BS, beam splitter; SM, silver mirror.

perfectly preserved for 500 ps. The period and contrast of a sine curve fitted to the measured beat are 8.02 fs and 0.93, respectively, almost the same as those of Fig. 4(a). Similar
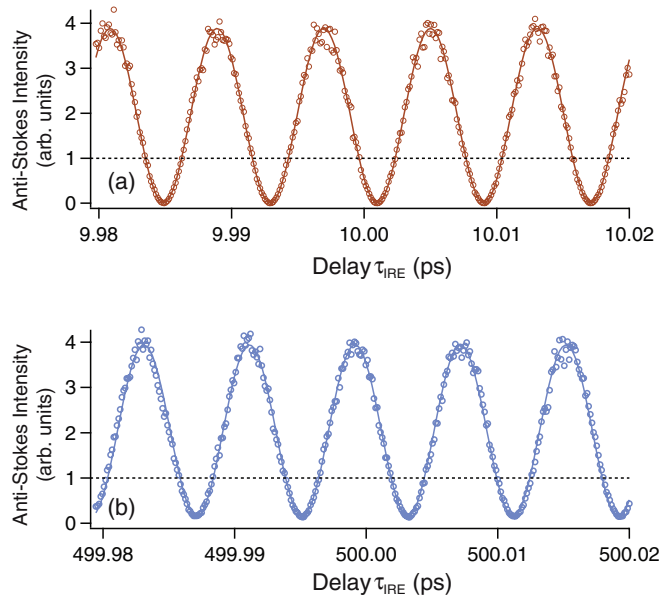

FIG. 4. (Color online) Quantum interferogram of the vibron state $|v = 1, \mathbf{k} = 0\rangle$ delocalized in solid p-H_2. The delay τ_{IRE} between the first and second pump-Stokes pairs is scanned around (a) 10 ps and (b) 500 ps. The solid curves represent sine functions least square fitted to the measured interferograms shown with open circles. The intensities of the anti-Stokes beam arising from a single pump-Stokes excitation are shown with the dashed horizontal lines for reference. The full range of each abscissa has been calibrated with a reference interferogram of He-Ne laser beams measured simultaneously.

interference has been observed in earlier multidimensional spectroscopic studies.[36] Here we have demonstrated such interferometry for the delocalized local excitations for the first time.

The high stability and resolution of our interferometer should enable us to keep the vibron interference locked to a particular single point in the vibron interferogram such as shown in Fig. 4. This locking experiment has been performed with the IRE delay τ_{IRE} feedback stabilized on the attosecond time scale. This feedback control was implemented so that the intensity of the reference He-Ne interferogram was kept constant. The stability of our interferometer has been evaluated from the drift of the spectral interferogram of the two pump pulses taken in another set of measurements shown in Fig. 5. It is seen that the drift of the spectrum seen in Fig. 5 was suppressed by the feedback control. The stability is thus estimated to be ± 15 as for ~6 min. This locked interference has been observed in real time with the probe delay τ_{probe} scanned from -10 ps to 1 ns.

Figure 6 shows the results of this locking experiment. The red and blue traces show the real-time evolutions of the vibron interference measured with two τ_{IRE}'s different from each other by 4 fs, whereas the black trace shows a reference taken with the second IREP blocked. It is clearly seen that the interference changes drastically from almost completely constructive (amplification by a factor of ~4) to destructive by changing τ_{IRE} by only 4 fs around $\tau_{IRE} = 500$ ps. The interference of delocalized local excitations in a bulk solid has been actively controlled, and its temporal evolution has been directly observed for the first time.

Recently, the importance of delocalized local excitations has been discussed extensively in a variety of subjects such as photosynthesis and quantum information processing. The
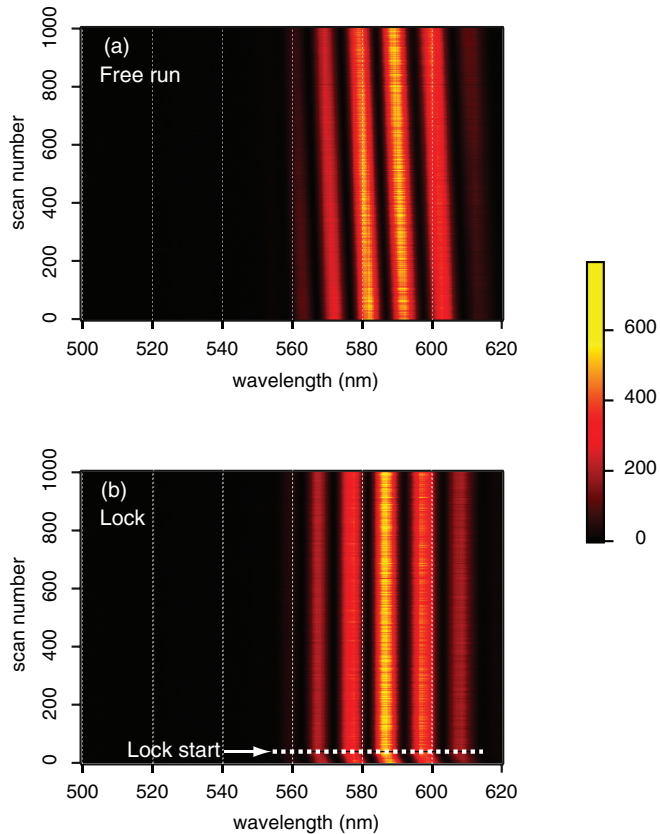
FIG. 5. (Color online) Feedback stabilization of the interferometer. The spectral interferogram of the two pump pulses produced from the interferometer was measured continuously for $\sim$6 min which corresponds to the full range of the ordinate (a) without the feedback control and (b) with the feedback control. The interpulse delay was set $\sim$100 fs.

spatiotemporal dynamics of the delocalized local excitations could be the origin of highly efficient energy transfer in a photosynthetic complex.[37] The delocalized local excitations in
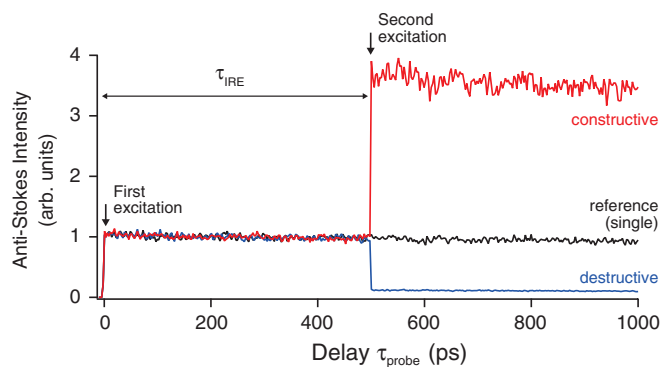

FIG. 6. (Color) Real-time observation of the actively controlled quantum interference of the vibron state $|v = 1, \mathbf{k} = 0\rangle$ delocalized in solid p-H_2. The delay τ_{IRE} between the first and second pump-Stokes pairs is different by 4 fs between the red and blue traces. The black trace shows a reference taken with the second pump-Stokes pair blocked. Each trace is an average of three repeated scans, and its vertical scaling is normalized by its intensities averaged over $\tau_{\text{probe}} = 0.7$–484.3 ps before the arrival of the second IREP.

an ultracold Rydberg gas gives Rydberg blockade interaction which is potentially useful to implement quantum gates among multiple atoms.[38,39] The present results suggest possibilities to control those systems coherently.

Our high-fidelity interferometry of delocalized wave functions is not specific to the vibrons of solid *para*-hydrogen. Instead it can be applied also to other delocalized local-excitations in a variety of molecular crystals, whose coherent lifetimes could be long enough for the conventional fs lasers.[40,41] Two phase-locked excitations in such interferometry can be spatially displaced to observe spatiotemporal evolutions of the wave functions in those bulk solids; the interference is expected to develop as the wave function produced by the first excitation becomes delocalized to be spatially overlapped with the second excitation. The coherence of this delocalized wave function could be actively distorted by an external field. We have established a method to distort vibrational coherence in an isolated molecule with a strong nonresonant fs laser pulse.[15] A similar method can be combined with our high-fidelity interferometry to simulate the localization of a delocalized wave function in a bulk solid.[42,43] There may be, however, better targets of such measurements than solid *para*-H_2, in which the dynamical evolutions may be too slow to be observed on our ultrafast time scales because of its extremely weak intermolecular interactions.

We have previously demonstrated logic gates with multiple eigenstates within the iodine molecule.[14,15] Amplitude and phase information of those eigenstates were retrieved sequentially by scanning an interrogating laser wavelength. Our present scheme, however, allows us to retrieve information from multiple eigenstates simultaneously by dispersing the anti-Stokes frequencies. Multiple eigenstates ($v = 1$, $J = 0$), ($v = 0$, $J = 2$), and ($v = 1$, $J = 2$) have been coherently excited by the present IREP although we focused on the pure vibrational state ($v = 1$, $J = 0$) in this paper. Those multiple eigenstates could be candidates for such multistate readout.

V. CONCLUSION

We have demonstrated direct observation and active control of quantum interference of delocalized vibrons in solid *para*-hydrogen. The technique developed for this active control is not specific to the vibrons of solid *para*-hydrogen. Instead it can be applied also to other delocalized wave functions in a variety of molecular crystals, and could be a useful experimental tool to explore spatiotemporal evolutions of delocalized wave functions in a bulk solid.

*Present address: Nara Institute of Science and Technology (NAIST); katsuki@ms.naist.jp

†ohmori@ims.ac.jp

[1] J. Frenkel, Phys. Rev. **37**, 17 (1931).

[2] G. D. Scholes and G. Rumbles, Nat. Mater. **5**, 683 (2006).

[3] P. Brumer and M. Shapiro, Chem. Phys. Lett. **126**, 541 (1986).

[4] D. J. Tannor, R. Kosloff, and S. A. Rice, J. Chem. Phys. **85**, 5805 (1986).

[5] T. C. Weinacht, J. Ahn, and P. H. Bucksbaum, Nature (London) **397**, 233 (1999).

[6] D. Meshulach and Y. Silberberg, Nature (London) **396**, 239 (1998).

[7] V. Blanchet, C. Nicole, M. A. Bouchene, and B. Girard, Phys. Rev. Lett. **78**, 2716 (1997).

[8] N. F. Scherer et al., J. Chem. Phys. **95**, 1487 (1991).

[9] T. Brixner, G. Krampert, T. Pfeifer, R. Selle, G. Gerber, M. Wollenhaupt, O. Graefe, C. Horn, D. Liese, and T. Baumert, Phys. Rev. Lett. **92**, 208301 (2004).

[10] M. P. A. Branderhorst, P. Londero, P. Wasylczyk. C. Brif, R. L. Kosut, H. Rabitz, and I. A. Walmsley, Science **320**, 638 (2008).

[11] E. W. Lerch, X. Dai, S. Gilb, E. A. Torres, and S. R. Leone, J. Chem. Phys. **124**, 044306 (2006).

[12] K. Ohmori, H. Katsuki, H. Chiba, M. Honda, Y. Hagihara, K. Fujiwara, Y. Sato, and K. Ueda, Phys. Rev. Lett. **96**, 093002 (2006).

[13] H. Katsuki, H. Chiba, C. Meier, B. Girard, and K. Ohmori, Phys. Rev. Lett. **102**, 103602 (2009).

[14] K. Hosaka, H. Shimada, H. Chiba, H. Katsuki, Y. Teranishi, Y. Ohtsuki, and K. Ohmori, Phys. Rev. Lett. **104**, 180501 (2010).

[15] H. Goto, H. Katsuki, H. Ibrahim, H. Chiba. and K. Ohmori, Nat. Phys. **7**, 383 (2011).

[16] H. Ibrahim, M. Héjjas, and N. Schwentner, Phys. Rev. Lett. **102**, 088301 (2009).

[17] T. Kiviniemi, J. Aumanen, P. Myllyperkiö, V. A. Apkarian, and M. Petterson, J. Chem. Phys. **123**, 064509 (2005).

[18] M. Fushitani, M. Bargheer, M. Gühr, and N. Schwentner, Phys. Chem. Chem. Phys. **7**, 3143 (2005).

[19] N. H. Bonadeo, J. Erland, D. Gammon, D. Park, D. S. Katzer, and D. G. Steel, Science **282**, 1473 (1998).

[20] M. U. Wehner, M. H. Ulm, D. S. Chemla, and M. Wegener, Phys. Rev. Lett. **80**, 1992 (1998).

[21] A. P. Heberle, J. J. Baumberg, and K. Köhler, Phys. Rev. Lett. **75**, 2598 (1995).

[22] M. Kuwata-Gonokami, R. Shimano, and A. Mysyrowicz, J. Phys. Soc. Jpn. **71**, 1257 (2002).

[23] D. Press, T. D. Ladd, B. Zhang, and Y. Yamamoto, Nature (London) **456**, 218 (2008).

[24] M. V. Gurudev Dutt et al., Science **316**, 1312 (2007).

[25] J. F. Sherson, S. J. Park, P. L. Pedersen, N. Winter, M. Gajdacz, S. Mai, and J. Arlt, New J. Phys. **14**, 083013 (2012).

[26] J. Van Kranendonk, Solid Hydrogen (Plenum, New York, 1983).

[27] T. Oka, Annu. Rev. Phys. Chem. **44**, 299 (1993).

[28] T. Momose, D. P. Weliky, and T. Oka, J. Mol. Spectrosc. **153**, 760 (1992).

[29] H. Katsuki, T. Nakamura, and T. Momose, J. Chem. Phys. **116**, 8881 (2002).

[30] I. I. Abram, R. M. Hochstrasser, J. E. Kohl, M. G. Semack, and D. White, Chem. Phys. Lett. **71**, 405 (1980).

[31] J. Z. Li, M. Katsuragawa, M. Suzuki, and K. Hakuta, Phys. Rev. A **58**, R58 (1998).

[32] C. Sierens, A. Bouwen, E. Goovaerts, M. De Mazière, and D. Schoemaker, Phys. Rev. A **37**, 4769 (1988).

[33] S. K. Bose and J. D. Poll, Can. J. Phys. **68**, 159 (1990).

[34] Solid p-H_2 takes hexagonal close packed (HCP) structure. An HCP lattice has two eigenstates for each **k** with even ($+$) and odd ($-$) symmetries under the inversion with respect to the center of two molecules within a unit cell. The $|v = 1, \mathbf{k} = 0\rangle$ state in the present paper represents the even eigenstate.

[35] S. Tam and M. E. Fajardo, Rev. Sci. Instrum. **70**, 1926 (1999).

[36] R. W. Schoenlein, D. M. Mittleman, J. J. Shiang, A. P. Alivisatos, and C. V. Shank, Phys. Rev. Lett. **70**, 1014 (1993).

[37] H. Lee, Y-C. Cheng, and G. R. Fleming, Science **316**, 1462 (2007).

[38] M. Reetz-Lamour, T. Amthor, J. Deiglmayr, and M. Weidemüller, Phys. Rev. Lett. **100**, 253001 (2008).

[39] D. Comparat and P. Pillet, J. Opt. Soc. Am. B **27**, A208 (2010).

[40] R. Kato, Y. Kawaguchi, and M. Ashida, Solid State Commun. **74**, 419 (1990).

[41] W. Guss, J. Feldmann, E. O. Göbel, C. Taliani, H. Mohn, W. Müller, P. Häussler, and H. U. ter Meer, Phys. Rev. Lett. **72**, 2644 (1994).

[42] W. H. Zurek, Rev. Mod. Phys. **75**, 715 (2003).

[43] A. Tonomura, J. Endo, T. Matsuda, T. Kawasaki, and H. Ezawa, Am. J. Phys. **57**, 117 (1989).